

Image sensors for radiometric measurements in the ocean

DESA E.S. and B. A. E. DESA

National Institute of Oceanography, Dona Paula, Goa - 403 004, India.

Abstract- This paper analyses the signal to noise (SNR) performance of selected linear array image sensors belonging to the CCD (charge coupled device), SSPDA (self scanning photodiode array), and PCD (plasma coupled device) families. Our purpose was to investigate image sensors for use in obtaining high resolution spectra of the upward and downward irradiance light fields in the ocean. Image sensors studied here, have practical dynamic ranges of the order of (10^4) . Given this, it is possible to work the sensors at a stabilised moderately cool temperature of 15 deg.C and to intelligently control the exposure time of the device, so as to reliably measure flux levels in the range $1\text{W/m}^2/\text{nm}$ to $10^{-6}\text{W/m}^2/\text{nm}$ commonly encountered in the ocean. The simulated response of each sensor type to a known in-situ spectrum is computed in terms of SNR values so as to narrow down the choice of sensor(s) for use in in-water radiometry.

INTRODUCTION

In the design and development of an in-water profiling radiometer for spectral irradiance measurements at sea, we were faced with the problem of selecting low light level detectors with a large dynamic range. The search for a suitable detector led us to a detailed examination of the new generation of commercially available image sensors.

In this paper, we examine the limiting signal to noise (SNR) performance of self-scanning photodiode arrays (SSPDA), plasma coupled devices (PCD), and linear charge coupled devices (CCD) as a function of exposure time, wavelength, temperature, irradiance, and depth of operation in the ocean. We begin by a comparison of image sensors suitable for use in optical radiometers followed by total noise estimates expected in selected image sensors. Variations in the functional dependence of SNR are computed, and discussed. The expected responses of different image sensors to a known in-water irradiance spectrum is computed so as to check pixel responses to actual field data. These computations indicate that the PCD image sensor is a good candidate for implementation in a profiling spectroradiometer. Our conclusions are summarised in last section.

RADIOMETRIC REQUIREMENTS OF THE DETECTOR

Before making a decision on the type of optical detector to use in the radiometer, it is instructive to list an ideal set of characteristics required of it. Having this in hand, we can begin to examine commercially available detectors that approach these requirements most closely.

Taking into account the problems faced in measuring irradiance (DESA and DESA 1989), a good detector should satisfy the following requirements:

- a) The spectral response should cover the spectral waveband 350nm to 750nm.
- b) In the ocean, irradiance levels can vary typically from $1\text{W/m}^2/\text{nm}$ at the sea surface to about $10^{-6}\text{W/m}^2/\text{nm}$ at a depth of 200 to 300 meters. The detector should therefore have an inherently large dynamic range $\sim (10^6)$.

c) High responsivity both in the blue (<440 nm) and red(680nm) regions of the in-water spectrum. This implies high quantum efficiencies (> 60%) and large aperture pixels on the image sensor.

d) Low dark signal at room temperature, so that the detector is not required to be cooled.

e) The detector must have a fast scan time so that surface wave noise perturbations on spectral irradiance data is minimised.

f) In the case of image sensors, the aspect ratio of the photo-sensitive area should be compatible with the image spectrum produced by the radiometric optics.

A cursory look at the characteristics of image sensors show that they satisfy nearly all of the above prerequisites. We have chosen to restrict our examination to linear array image sensors only, leaving aside other optical detectors e.g. area array image sensors, photomultipliers, vidicons and single element photocells. For the radiometric application here, image sensors can be conveniently coupled to fixed grating spectrographs, eliminating the use of moving parts in a sea based instrument package.

SENSORS AND THEIR COMPARISONS

Silicon based image sensors are manufactured using several different technologies. This has produced the self scanned photodiode arrays (SSPDA), the charge coupled device (CCD), the charge injection device (CID), and the less well known plasma coupled device (PCD).

Perhaps the best known member of the image sensor family is the CCD, primarily due to the fact that early developmental efforts on them were directed to using them for commercial solid state TV cameras in high signal/noise environments. Scientific applications, on the other hand, invariably require optical detection in low signal to noise conditions and this entails the use of scientific grade image sensors with low readout noise, high quantum efficiency, large dynamic range, excellent linearity, and wide spectral bandwidth.

A shortlist of the most likely image sensors for use in low light level spectroscopy in the ocean can be compiled by selecting those sensors with a high responsivity and large quantum efficiencies across the visible spectrum. Responsivity (R) is defined as the signal charge (Coulombs) stored on a pixel per unit of exposure (Joules/m²) where the exposure is the irradiance multiplied by the integration time. The units of responsivity are Coul/Joule/m² (C/J/m²) and it can be written as:

$$R = Q / (I.t) \quad \dots(1)$$

where Q is the signal charge on a pixel (Coulombs), I is the irradiance (W/m²/nm), and t is the integration or exposure time (seconds). Graphically, responsivity or sensitivity is the slope of the straight line plot between the signal charge Q with exposure. The quantum efficiency (QE) is related to R, the responsivity by the relation :

$$QE = R.h.c / (\lambda .A.q) \quad \dots(2)$$

where h and c are Planck's constant and the velocity of light respectively, λ is the wavelength of a photon, A is the pixel aperture and q is the electronic charge. Equation 2 indicates that an image sensor with a large pixel area, and a large QE will have a high responsivity value. That this is true can be seen in Table 1. In the selection of devices, we looked at SSPDA's from EG&G reticon, CCD's from Thomson CSF and Tektronix, and PCD's from Hamamatsu having high R values. The signal to noise dependence on exposure time, wavelength, and irradiance level will be computed for the devices 1,2, & 3 listed in Table 1, after a consideration of the noise sources in these device types.

Table 1. Comparing image sensors at 25°C

Device Type	Pixel Size	Responsivity C/J/m ² @ 650nm	QE (%) @440nm	Dynamic Range	Dark Current (pA)	Reset Cap. (pF)	Saturation Electrons
SSPDA T-series RETICON	50u x 2500u	5.24x(10 ⁻⁸)	68	10 ⁴	10	4	1.75x(10 ⁸)
CCD TH7831 THOMSON	13u x 39u	4.0x(10 ⁻¹⁰)	95	10 ³	.0064	0.08	1.43x(10 ⁶)
PCD S2301 HAMAMATSU	36u x 2500u	3.33x(10 ⁻⁸)	56	10 ⁴	2.0	4	1.25x(10 ⁸)
AREA CCD TK 512	27u x 27u	1.44x(10 ⁻¹⁰)	35	10 ⁴ (?)	0.05	-	> 4x(10 ⁵)
SR SERIES RETICON	25u x 2500u	2.50x(10 ⁻⁸)	68	--	0.50	4	6.25x(10 ⁷)

NOISE CONSIDERATIONS IN IMAGE SENSORS

Noise (measured in electrons) consists of undesirable signals from various sources in the image sensor and imaging system. As our main objective is to obtain an overall trend in device performance, we shall limit our calculations to accounting for the major sources of noise common to most image sensor types. The major noise sources are:

- * Photon shot noise,
- * Dark current noise,
- * Reset noise and amplifier noise.

Before discussing these noise contributions, it is necessary to note the existence of fixed pattern noise, which has been neglected in our calculations for reasons explained below. There are basically two types of fixed pattern noise (FPN) to consider, namely dark signal non-uniformity (DSNU) and the noise from switching clock transients.

Fixed Pattern Noise (FPN)

Dark signal non-uniformity (DSNU)

This noise source is time independent and temperature dependent, and arises from local crystal defects or inhomogeneities in the silicon substrate of the device. It imposes a limit on the smallest possible signal that can be detected by the device. DSNU follows the same temperature law as the average dark current, and a rough guess will be typically 10% of the average number of dark electrons. Devices with high quality substrates having near zero defects will have negligible DSNU. Every image sensor will have its characteristic DSNU signature in the absence of light. One would be led to expect that DSNU could be subtracted out provided the device is run at a fixed stable temperature, however detailed specifications on DSNU and its temperature dependence are in most cases not available.

Noise from switching clock transients

The second type of FPN common in most image sensors is time and temperature independent. It is caused by spurious transients coupled into the video line when alternate pixels (or diodes) are sampled by different clock phases. A lack of coincidence in the switching edges of the clocks used in opening and then closing successive switches in the shift register of the device results in a switching transient. Under constant conditions of operation, this source of FPN is removable by subtracting a dark scan from a real scan, and can be minimised considerably by good circuit layout.

Photon shot noise is a consequence of the corpuscular nature of light. The photons generated by a steady light source obey Poisson statistics. The conversion of photons to electrons by the photosensor pixel induces the same Poisson distribution in electrons. The noise associated with this process is equal to the square root of the signal ($\sqrt{N_p}$) where N_p is the number of electrons generated in a pixel of the image sensor.

Dark current noise ($\sqrt{N_d}$) is generated by the collection of charges from thermal processes in silicon devices, and it has a strong temperature dependence. It is expressed as:

$$N_d = \sqrt{i_d t / q} \quad \dots(3)$$

where i_d is the dark current, t is the exposure time between read scans of the device, and q is the electronic charge. As a rule of thumb, i_d doubles for every 7°C increase in temperature. Typically i_d is less than 10 nA/cm² at 25°C for scientific grade devices.

Reset noise (N_r) arises from resetting a pixel to its reference potential. The r.m.s value is given by:

$$N_r = \sqrt{(kTC)/q} \quad \dots(4)$$

where k is Boltzmann's constant, T is the absolute temperature ($^{\circ}K$), and C is the pixel (diode) capacitance (or the readout capacitance in CCD's). Reset noise is also temperature dependent. Typical capacitance values in CCD's are 0.1pF, and in SSPDA's and PCD's it is 20~ 50pF (see device data books).

Amplifier noise (N_a) depends on the amplifier used i.e., the bandwidth, input capacitance, and the stray capacitance to the amplifier input node (Simpson 1979). Selection of low noise components for the amplifier are important. A low video line capacitance makes it possible to achieve a low noise figure. For Reticon arrays $N_a < 1000$ electrons, and for Thomson CCD's $N_a \sim 150$ electrons. Amplifier noise is temperature dependent.

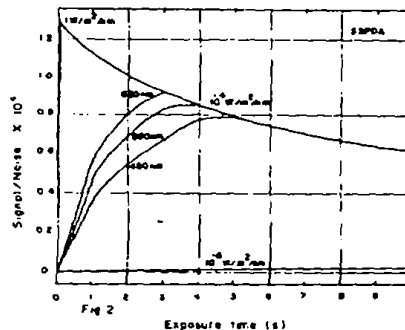
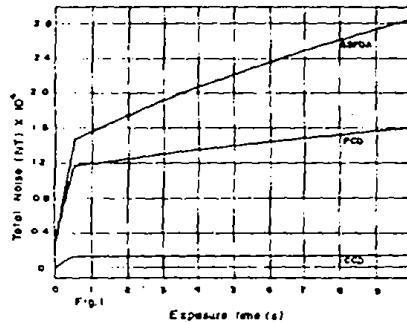


Fig. 1. Total noise changes of SSPDA,PCD, and CCD sensors with exposure time. Constants in the calculation are $I = 1W/m^2/nm$, at wavelength 550nm & $T = 298 K$.

Fig. 2. SNR dependence on exposure time for EG&G Reticon SSPDA for $I = 1, 10^{-4}$, and $10^{-6} W/m^2/nm$ at $T = 298K$.

Total Noise (N_t) Taking only the major noise sources into account, the total noise N_t can be expressed as:

$$N_t = \sqrt{(N_p + (N_d)^2 + (N_r)^2 + (N_a)^2)} \quad \dots(5)$$

The exposure time (t) dependence of N_t results from the dark current noise term (N_d) in (3). N_t is also a function of irradiance level through the photon noise term $\sqrt{(N_p)}$, and to temperature T through the terms N_d , N_r and N_a . Setting the irradiance and the temperature as constants, the total noise N_t for the SSPDA, CCD, & the PCD is plotted against the exposure t in Fig 1. As expected N_t grows with increasing exposure times t . The noise level of the CCD is the lowest because the dark current(.0064pA) and the reset capacitance (.08pF) are small.

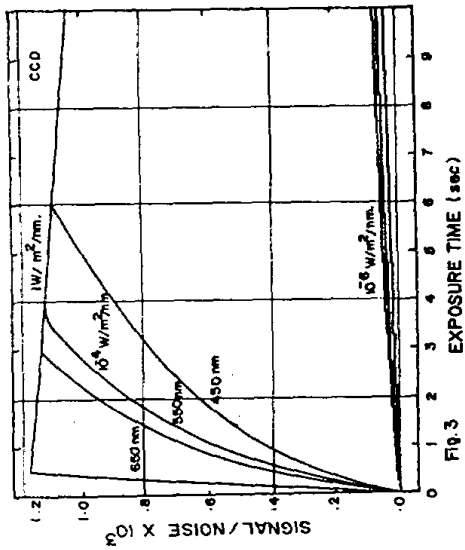


FIG. 3

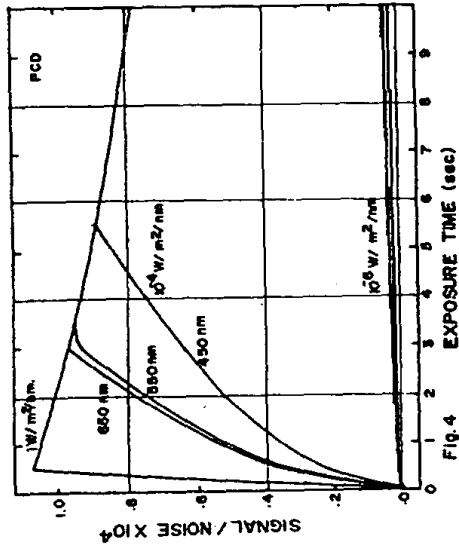


FIG. 4

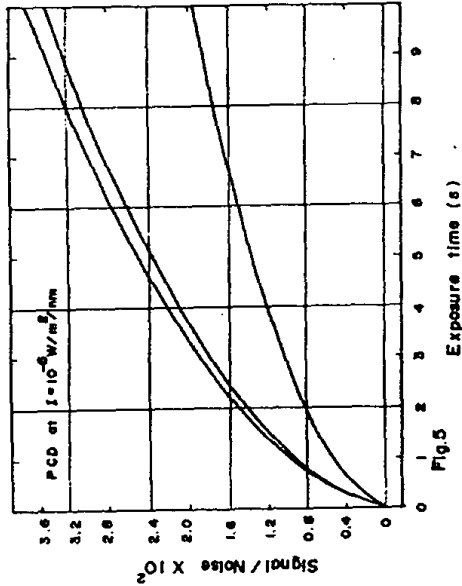


Fig. 5

Figs. 3 & 4. SNR changes with exposure time for Thomson TH 7831 CCD and Hamamatsu S2301 PCD sensors respectively for $I = 1, 10^{-4}$ and $10^{-6} \text{ W/m}^2/\text{nm}$ at $T = 298\text{K}$.

Fig. 5. Expanded view of SNR with exposure time for Hamamatsu PCD sensor at irradiance level of $10^{-6} \text{ W/m}^2/\text{nm}$, $T = 298 \text{K}$, and at three wavelengths 650, 550 and 450 nm.

SIGNAL / NOISE (SNR) DEPENDENCE ON EXPOSURE TIME

The SNR of an image sensor is simply:

$$\text{SNR} = N_p / N_t \quad \dots(6)$$

Figs. 2,3 and 4 show the room temperature SNR dependence of the SSPDA, CCD, and PCD sensors on the exposure time respectively. All three graphs show a rapid increase of SNR to the saturation charge level of the pixel within a few milliseconds at high ir radiance ($1\text{W}/\text{m}^2/\text{nm}$). Further increases of SNR at large t are not possible as the device is at saturation with the noise N_t increasing. Thus SNR shows a decreasing trend at high light fluxes. The graphs in Figs. 2 to 4 show a wavelength dependence of the SNR at lower values of the irradiance level. Red photons at 650nm produce higher SNR values than do blue photons at 450nm in all devices studied. This is as expected because the responsivity is maximum at 750nm for most silicon based image sensors.

At irradiance levels of $10^{-6} \text{W}/\text{m}^2/\text{nm}$, the shape of the SNR curves shows an approximate parabolic increase with exposure time. An expanded view of the 10^{-6} curves of the Hamamatsu PCD sensor (Fig.4) is redrawn to full size in Fig.5. Even at this low flux level, there exists enough signal to noise to reliably digitise & record a spectrum. By using larger exposure times, and averaging several scans of the spectrum, the SNR can be increased by a large factor. The SNR curves have all been computed at 298°K . Calculations repeated at lower temperatures would all show larger SNR values. We observe from Fig.5 that most of the increase of SNR occurs within the first second of exposure time. This appears consistent with the total noise dependence with exposure time (see Fig.1).

At flux levels of $10^{-8} \text{W}/\text{m}^2/\text{nm}$, the SNR dependence for the PCD sensor is plotted in Fig.6. At this irradiance level, signal to noise ratios are approximately unity, and it is safe to assume that the limits on device performance have been reached, and further manipulations on temperature or exposure time will not improve the signal to noise ratio.

SIGNAL /NOISE DEPENDENCE ON WAVELENGTH

The signal to noise curves with exposure time computed in Figs. 2,3 and 4 indicate a dependence on wavelength. This is expected, as the responsivity of an image sensor pixel is wavelength dependent. In order to verify this more closely, and because our primary interest is in detectors for radiometry, the SNR of a T-series SSPDA (see Table 1) as a function of wavelength at constant depths in the ocean is shown in Fig.7. The curves have been drawn using the attenuation coefficients of pure seawater (SMITH and BAKER, 1978) and the simple exponential law relating the irradiance $I(z,\lambda)$ at depth z and wavelength λ to the surface irradiance I_0 (Beer's Law):

$$I(z, \lambda) = I_0 \cdot \exp [-K(z,\lambda) \cdot z] \quad \dots(7)$$

therefore

$$\text{SNR} = R(\lambda) \cdot I(z, \lambda) \cdot t / (q \cdot N_t) \quad \dots(8)$$

where I_0 is taken as $1\text{W}/\text{m}^2/\text{nm}$ at the sea surface ($z=0$), $K(z,\lambda)$ is the diffuse attenuation coefficient, and $t = 50 \text{ms}$. The SNR dependence on wavelength (Fig.5) is idealised, but it shows that the blue (350nm) and red (650nm) parts of the in-water spectrum show large changes in SNR over relatively small depth changes. The peak at the blue wavelength 450nm has the largest SNR at all depths. At shallow depths (0 to 50 meters) where the irradiance signal is large, the image sensor will have to be run at very short exposure times (<50 ms) to avoid signal saturation seen in Fig.7

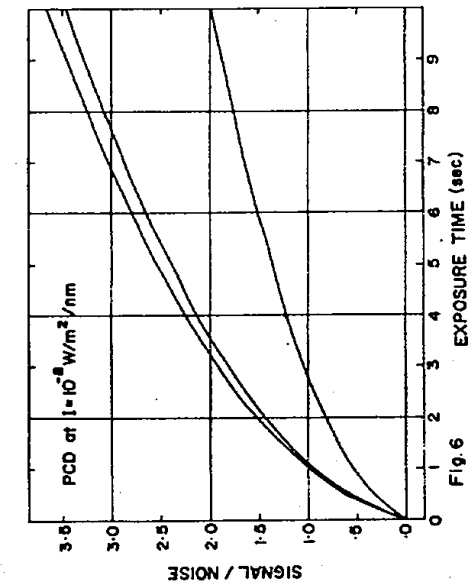


Fig. 6

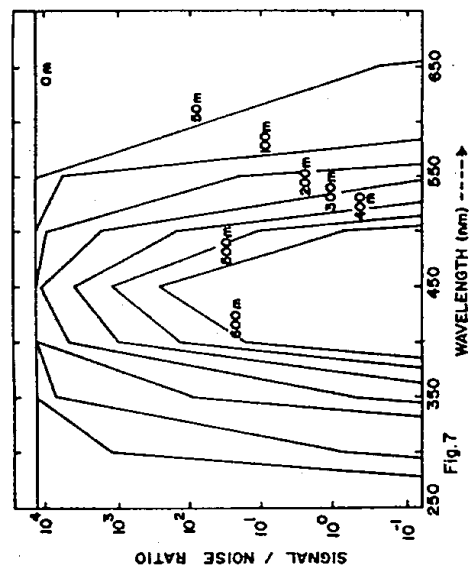


Fig. 7

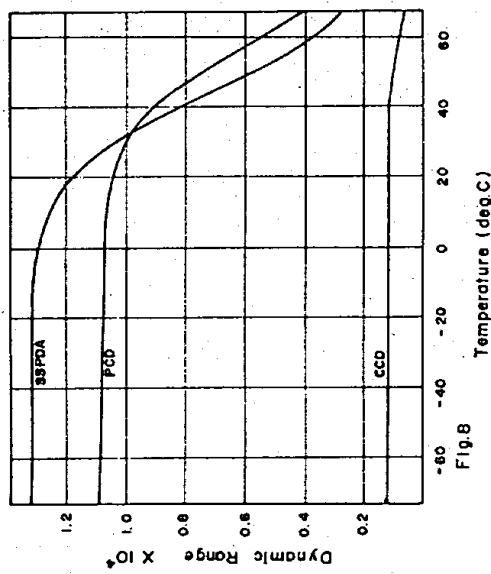


Fig. 8

- Fig. 6. SNR with exposure time for PCD sensor but at irradiance of $10^{-8} \text{ W/m}^2/\text{nm}$ and other conditions as in fig.5
- Fig. 7. Idealised behaviour of SNR with wavelength for pure seawater at different depths. Constants are exposure time of 50 ms and $T = 298 \text{ K}$.
- Fig. 8. Dynamic Range changes with temperature for SSPDA, PCD and CCD sensors at constant exposure of 1 sec. and irradiance of $1 \text{ W/m}^2/\text{nm}$.

DYNAMIC RANGE

This quantity is defined here as the maximum signal to noise ratio. The largest value that can be read off the graphs of Figs. 2,3, and 4 is the dynamic range for that device. (see also Table 1). In the measurement of irradiance in the ocean, it is useful to distinguish between dynamic range caused by changes in irradiance in a single scan across the spectrum, and that caused by changes in irradiance with depth at a fixed wavelength.

Rough estimates of dynamic range (DR) in terms of signal to noise can be obtained from the idealised curves of Fig.7. Choosing the 50 meter profile shows that DR from the peak wavelength (450 nm) to the red (650nm) is approximately 10^4 . Similarly at the fixed worst case wavelength at 650nm, the DR with depth is approximately 10^4 .

Alternatively, we can estimate dynamic range in terms of irradiance levels ($W/m^2/nm$) using the well known ideal exponential law for irradiance (equation 7). It turns out that irradiance levels can vary from $(10^{-1})W/m^2/nm$ to $(10^{-8})W/m^2/nm$ across the 50 meter spectrum, and from $1W/m^2/nm$ to $(10^{-6})W/m^2/nm$ in going from the surface to depth at 180 meters at 450nm. As a rough indicator of the real effect, we can expect that irradiance levels will change typically, by about six decades subject to other factors such as the water type, solar elevation, pigment content, and the condition of the sky and the sea. In summary, a device with a dynamic range of 10^4 , should be capable of measuring a corresponding 10^6 change in irradiance flux.

Upper limit on dynamic range

The maximum possible value of the dynamic range of the SSPDA, CCD, and PCD devices listed in Table 1 can be estimated from the SNR curves. The maximum DR can be expressed as the ratio of the total number of electrons at saturation, to the minimum value of the total noise N_t , in the limit when the dark noise N_d and reset noise N_r tend to zero at very low temperatures and very short exposure times. The approximate maximum DR values for the devices are:

$$\begin{aligned} \text{SSPDA} &: \text{DR} = 7 \times 10^4 \\ \text{CCD} &: \text{DR} = 7.6 \times 10^3 \\ \text{PCD} &: \text{DR} = 5.5 \times 10^4 \end{aligned}$$

In practice, DR values will be a factor of 3 less than the ideal maximum, because of the finite dark noise, and the other noise sources described in the preceding sections. Marginally higher DR values can be obtained if the devices are run at short exposure times (<1 s). Cooling the device can also increase the DR of the device. The effect of temperature on DR is shown in Fig.8 for constant exposure time of 1s, and irradiance flux level of $1W/m^2/nm$. Interestingly, the DR does not show a significant increase for temperatures below 20°C . The flattening effect of DR at temperatures below zero centigrade shows that the pixels on the sensor have reached saturation, with only small changes in total noise N_t . The use of a miniature solid state thermoelectric cooler with closed loop temperature control could be used to maintain the image sensor at a constant temperature. It is seen from Fig. 8 that only moderate cooling to 15°C would be necessary for *in-situ* radiometry. A constant temperature on the image sensor would minimise drifts in dark noise fluctuations, and reset noise, allowing these factors to be better defined and subtractable in extreme cases.

SIGNAL TO NOISE RESPONSE TO A REAL SPECTRUM

Using the results of the preceding sections it is possible to compare the SNR output of the SSPDA, PCD and CCD devices (devices 1,2, and 3 of Table 1) to a known low light level *in-situ* spectrum. It is assumed that the spectrum is made to fall on the

device directly. The spectrum chosen (see Fig.9) is a downward irradiance spectrum measured by Okami and Kishino (1981) at a depth of 15 meters in Tokyo Bay. The peak value is $1.063 \times 10^{-3} \text{ W/m}^2/\text{nm}$ at 580nm, and the extreme blue (450nm) and red (650nm) ends fall to a value of $5 \times 10^{-5} \text{ W/m}^2/\text{nm}$.

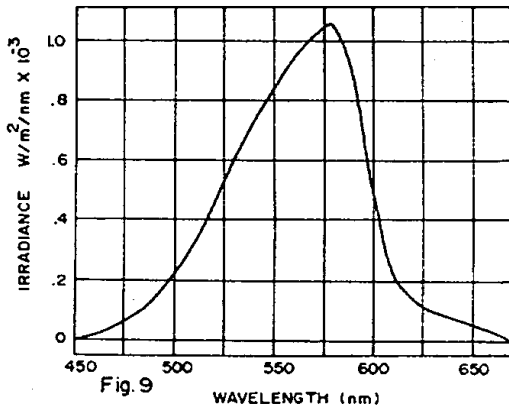


Fig. 9

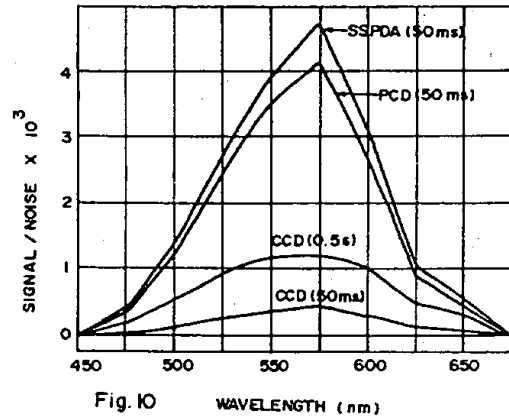


Fig. 10

Fig.9. *In-situ* irradiance spectrum from Tokyo Bay. Units are in $\text{W/m}^2/\text{nm}$.

Fig.10. Computed signal to noise response for the SSPDA,PCD, and CCD image sensors corresponding to the *in-situ* downward irradiance spectrum of Fig.9. The exposure time was fixed at 50ms.

The SNR response of the devices are compared in Fig.10 using a fixed exposure time of 50ms and a pixel bandpass of 2nm. As expected, the SSPDA and PCD have closely similar responses with peak SNR's of the order of 4500. The CCD sensor with smaller pixel dimensions, and lower responsivity shows a correspondingly lower SNR ~ 400.

The effect of increasing the exposure time of the device is equivalent to changing the gain of the spectral signal without the need of extra circuitry. Software algorithms can be written to adaptively control the exposure time. The linear response of image sensors as expressed in equation 1 means that changes in exposure time will not produce any distortion in the shape of the spectrum provided the device is run below saturation levels. The effect of increasing the exposure time from 50ms to 500ms for the CCD sensor can be seen in Fig.10. Saturation at the peak is evident. Similarly, the SSPDA and PCD saturate at exposure times of 1s. Clearly, device performance can be exploited at light levels as low as $(10^{-8}) \text{ W/m}^2/\text{nm}$. At high light levels of $1 \text{ W/m}^2/\text{nm}$, neutral density filters, and short exposure times would be necessary to prevent device saturation.

SUMMARY

This paper has examined the signal to noise behaviour of selected image sensors for use in radiometry of the ocean. We conclude that scientific grade image sensors examined here, have dynamic ranges of 10^4 , which adequately cover irradiance flux changes from $1 \text{ W/m}^2/\text{nm}$ to $10^{-6} \text{ W/m}^2/\text{nm}$. At irradiance levels of $10^{-8} \text{ W/m}^2/\text{nm}$, the limits on device performance have been reached. In using image sensors for *in-situ* radiometry, care must be taken in selecting sensors with high responsivity in the blue and red regions of the photosynthetic spectrum, with large pixel apertures, low total noise, low DSNU, and large dynamic range. Our calculations indicate that such devices should be run at moderate constant temperatures so that drifts are kept to a minimum.

Intelligent control of the SNR of the device under different irradiance levels using short or long exposure times whenever necessary, coupled with spectral scan averaging are all necessary techniques to fully exploit image sensor performance.

Acknowledgments - The authors wish to thank Prof. G.S.HOBSON, EURICO D'SA, and R.G. PRABHU DESAI for taking time to discuss image sensors, and the Director, National Institute of Oceanography for the liberal use of laboratory facilities. The work is part of a project funded by the United Nations Development Programme, and the Govt. of India.

REFERENCES

- CCD DATA BOOK (1989). Thomson Composants Militaires et Spatiaux, France.
- DESA E.S. and B.A.E.DESA (1989) The design of an in-water radiometer. *Oceans* 89. 3, 998-1003.
- IMAGE SENSING PRODUCTS (1989) CATALOG. EG&G Reticon, Sunnyvale, California, USA.
- MOS LINEAR IMAGE SENSORS (1990) CATALOG. Hamamatsu Photonics K.K., Solid State Division, Japan.
- OKAMI.N.,M.KISHINO,S.SUGIHARA and S.UNOKI (1981). Measurements of spectral irradiance in Tokyo Bay. *The Institute of Physical & Chemical Research (RIKEN). Technical Report No.5.* p20.
- SIMPSON.R.W.(1979). Noise in large aperture self-scanning diode arrays. *Review of Scientific Instrumentation* 50(6).
- SMITH R.C. and K.S.BAKER (1978) Optical classification of natural waters. *Limnology and Oceanography* 23, 260-267.